

Curcumin Ameliorates Obesity Associated Disorders in High Fat-Fed Male Albino Rats: Role of Hepcidin

Original Article *Amal Fawzy¹, Radwa Mahmoud², Safia Ibrahim², Abeer A. Mahmoud³ and Walaa Samy¹*

¹Department of Medical Biochemistry, ²Department of Physiology, ³Department of Medical Histology and Cell Biology, Faculty of Medicine, Zagazig University, Egypt

ABSTRACT

Introduction: In developed countries, obesity and iron deficiency are frequently encountered nutritional disorders. Nonalcoholic fatty liver disease (NAFLD) is a global health problem. Hepcidin is a peptide produced mainly by hepatocytes and adipocytes, which are responsible for iron metabolism, immunity, and inflammatory regulation. Curcumin, the active ingredient of turmeric.

Aim of the Work: Assess the role of hepcidin in iron homeostasis and its effects on fatty liver in albino rats with HFD-induced obesity. Also explore the protective role of curcumin on hepcidin-related obesity associated disorders.

Materials and Methods: Thirty adult male albino rats were divided into three groups: group I: consumed normal diet, group II: consumed high-fat diet (HFD) and group-III curcumin-treated group was fed a high-fat diet supplemented with curcumin. Body Mass Index (BMI), abdominal circumference (AC), lipid profile & some iron parameters were measured. Also, adipose-tissue-expressed hepcidin, interleukin 6 (IL-6), and tumor necrosis factor- α (TNF- α) were measured by real-time polymerase chain reaction (PCR). Hepatic tissues were stained with hematoxylin and eosin (H&E), Masson trichrome (MT) and examined microscopically. Expression levels of BAX proteins were detected by immunohistochemistry.

Results: The HFD significantly stimulated adipose tissue expression of hepcidin, IL-6, and TNF- α . The HFD group had low serum iron, transferrin saturation levels and high serum ferritin. There was a significant correlation between hepcidin expression in adipose tissue and IL-6 and TNF- α expression in the HFD group. Non-alcoholic fatty liver was also identified in HFD-induced obesity group. Treatment with curcumin significantly improved the above mentioned parameters.

Conclusion: Hepcidin expression in dipose tissue plays a significant role in functional iron deficiency and non-alcoholic fatty liver in obese albino rats that are improved by curcumin which has antiobesity, antioxidant, and anti-inflammatory effects.

Received: 31 July 2022, **Accepted:** 06 October 2022

Key Words: Adipose tissue, curcumin, hepcidin, iron, obesity.

Corresponding Author: Abeer A. Mahmoud, PhD, Department of Medical Histology and Cell Biology, Faculty of Medicine, Zagazig University, Egypt **Tel.:** +20 10 0405 5839, **E-mail:** abeerazeem@hotmail.com

ISSN: 1110-0559, Vol. 46, No. 4

INTRODUCTION

Obesity is a health issue that is related to several metabolic diseases, especially nonalcoholic fatty liver disease (NAFLD), cardiovascular risk, dyslipidemia, insulin resistance (IR) and type II diabetes^[1,2].

Non-alcoholic fatty liver disease (NAFLD) refers to a variety of disorders caused by excessive fat accumulation in the liver, which may proceed to nonalcoholic steatohepatitis (NASH), fibrosis, cirrhosis, and even hepatocellular carcinoma. According to estimate 25% of people globally have NAFLD and continues to rise with the obesity epidemic worldwide^[3].

Many obesity-related disorders are attributed to low-grade inflammatory reactions triggered by stretched fatty tissue. This stretching releases many inflammatory cytokines, such as interleukin-6 (IL-6) and tumour necrosis factor (TNF), that harm several non-adipose tissues^[4].

Hepcidin is a peptide hormone released by liver cells and is responsible for regulating iron metabolism, immunity,

and inflammatory processes. It is well known that hepcidin cause down regulation of iron homeostasis by preventing macrophages from releasing recycled iron from aged red blood cells and dietary iron absorption by enterocytes^[5]. The effect of iron on liver inflammation occurrence has become a point of interest in many experimental studies, where iron homeostasis disturbance may play a role in NAFLD^[6,7].

Although hepcidin is expressed mainly in the liver, however studies indicate that it can also be expressed in macrophages and adipose tissue in inflammatory states. Some researches done on children and teenagers report an iron deficiency secondary to obesity associated with elevated levels of hepcidin^[8,9].

Pathologically elevated hepcidin concentrations cause or exacerbate iron-restrictive anemias such as anemias associated with inflammation, chronic kidney disease and some malignancies. Hepcidin deficiency results in iron overload in hereditary hemochromatosis and inefficient erythropoiesis. The hepcidin-ferroportin axis is the main

regulator of extracellular iron homeostasis in health and disease, and is a prospective target for the diagnosis and treatment of iron disorders and anemias^[9,10].

Curcumin, a naturally occurring polyphenolic molecule with anti-inflammatory, antioxidant, and hepatoprotective roles. Curcumin has been demonstrated to protect the liver from storage of fat brought on by a high-fat diet in recent animal studies^[11,12].

AIM OF THE WORK

The current work aimed to study hepcidin's role in iron homeostasis, and effects on a high-fat diet (HFD) induced obesity-associated disorders, such as functional iron deficiency anemia, NAFLD, and curcumin protective effects.

MATERIAL AND METHODS

This was done at Faculty of Medicine, Zagazig University in a period from January to July 2019. The study involved a local strain of 30 healthy adult male albino rats (151–190 gm) from the Veterinary Medicine Animal House. Rats were housed in clean steel wire cages (5/cage) with a natural light/dark cycle, and with free water access. Food was obtained from the Faculty of Agriculture, Zagazig University. The Institutional Research Board and Ethics Committee of Faculty of Medicine, Zagazig University approved the work protocol.

Three groups each contained 10 rats were designed:

Group (I) control group: normal fed diet, which received 3.41 kcal/g of normal chow diet for 12 weeks. Calories were distributed as follows: 6% fat, 17% proteins, and 77% carbohydrates^[13].

Group (II) high-fat-diet-induced obesity group: received 5.6 kcal/g of a HFD for 12 weeks. Calories were distributed as follows: 58% fat, 18% proteins, and 24% carbohydrates^[14]. The food iron content was the same for both food groups.

Group (III) curcumin group was received a high-fat diet with curcumin 0.1 percent for 16 weeks. According to earlier research Hasan et al., demonstrated that curcumin at the medium dose of 0.05-0.1 percent was efficient at lowering levels of numerous inflammatory cytokines^[15,16]. Curcumin (purity: 98 percent) was purchased from Sigma-Aldrich (St. Louis, MO, USA).

The food iron content was the same for both food groups

A 25 mg/kg intraperitoneal dose of sodium thiopental was used to anaesthetize rats. At the conclusion of the study, blood samples from the retro-orbital plexus were taken. Rats were sacrificed, the abdominal cavity was opened, and visceral adipose tissue (perirenal, omental, and mesenteric) was removed and kept at 80°C until gene expression could be assessed. The livers were separated and cleansed. Each isolated liver was split into two pieces. For histological analysis, the first portion was fixed in neutral formalin

solution at a 10% concentration. The second part was homogenized and then centrifuged. For measurements of malondialdehyde (MDA), lipid peroxidation, and hepatic iron concentration (HIC), the supernatant was taken and transferred to another tube.

Anthropometric measurements

Body weight was measured by a digital balance at time zero, and then again after 12 weeks. The nose to anus length was measured according to Novelli 17. The formula used to determine Body Mass Index (BMI) was: BMI = Body Weight (gm)/Length (cm²). The obesity cut off value was BMI > 0.68 gm/cm²^[17]. The abdominal circumference (AC) was measured at the widest zone with a plastic tape measure^[18].

Blood Sample

Blood was drawn from the retro-orbital venous plexus and placed into two microcentrifuge tubes: one with an anticoagulant [ethyl-enediamine tetra acetic acid (EDTA, K2)], and the other with a serum separator. Hemoglobin concentration (Hb), hematocrit value (PCV), and mean corpuscular hemoglobin (MCH), were measured in the anticoagulant samples using an automatic blood analyzer (Coulter LH 750 Hematology Analyzer). Clotted serum samples were obtained by centrifugation for 20 min at 3000 rpm and frozen at (-20°C) until assayed.

Biochemical analysis

Serum levels of lipid were assessed. Low-density lipoprotein-cholesterol (LDL-C) and very-low-density lipoprotein-cholesterol (VLDL-C) were estimated. All measurements were performed using BioSource Europe S.A. Belgium kits. Total serum cholesterol (TC) was measured using the Tietz^[19] method. The Fossati and Prencipe^[20] enzymatic colorimetric method was adapted to measure triglyceride (TG). HDL-C serum levels were measured following the Nauk^[21] method. The LDL-C serum levels were calculated by the Friedewald^[22] equation: LDL-C = TC -HDL-TG/5. VLDL-C levels in serum were also calculated by the Friedewald^[22] equation.

Hepatic parameter measurements

The Rec^[23] method was adopted to measure both serum aspartate aminotransferase (AST) and alanine aminotransferase (ALT) levels using AST & ALT ELISA rat kits (Shanghai Sun Red Biological Technology, China). Albumin level in serum was calculated by the method Stoskopf^[24] using the bromocresol green. Rat serum hepcidin was measured using ELISA kits (USCN life Co., Houston, TX, USA) following the manufacturer's instructions^[25]. TNF- α and IL-6 were estimated by ELISA (USCN life Co., Houston, TX, USA) according to the manufacturer's instructions^[26]. Serum iron (SI) and the total iron-binding capacity (TIBC) were measured using the Burits and Ashwood^[27] technique and commercially available kits. The transferrin saturation percentage (TS %) was estimated using the ratio of SI and the TIBC

as presented by Siff et al.^[28]. Hepatic iron concentration (HIC) was estimated according to the manufacturer's instructions^[29] by the Tissue iron assay kit (Abcam, Cambridge, MA, USA). MDA liver concentrations were measured by a lipid peroxidation assay kit (Cayman, Ann Arbor, MI, USA).

Detecting Hepcidin, IL-6, and TNF- α gene expression by real-time Polymerase Chain Reaction (real-time PCR) in rat adipose tissue

Total RNA from adipose tissue was extracted using the RNeasy Lipid Tissue Mini Kits. The total RNA concentration was measured by 260/280 nm absorbencies. QuantiTect SYBR Green RT-PCR kits (Qiagen,) were

used to produce complementary DNA (cDNA) from the extracted RNA by reversed transcription. Glyceraldehyde-3-phosphate dehydrogenase (GAPDH) used as an internal control. List of primers is in (Table 1). The PCR was done in a total of 25 μ l: 12.5 μ l QuantiFast SYBR Green PCR Master Mix, 1 mM of each primer (Invitrogen, USA), and 2 mL cDNA. The PCR settings were: 30 cycles of 1 min at 95°C for denaturation, 1 min at 60°C for annealing, and extension for 1 min 30 s at 72°C. The final step consisted of an extension step for 10 min at 72°C. All primer sets had a calculated annealing temperature of 60°C. The hepcidin, IL-6, and TNF- α expression were calculated using the comparative Ct method formula $2^{-\Delta\Delta Ct}$. All kits were from QIAGEN (Valencia, CA, USA)

Table 1: primer sequence for hepcidin, IL-6, TNF- α , and GAPDH genes

	Forward primer	Reverse primer
hepcidin	5'CAAGAT GGCCTAAG CA TCG 3'	5'-GCT GGG GTA GGA CAG GAATAA -3'
IL-6	5'GGGACTGATGTTGTTGACAG 3'	5'TGTTCTTCACAAACTCCAGG 3'
TNF- α	5'CCCAGACCCTCACACTCAGAT3'	5'TTGTCCCTGAAGAGAACCTG 3'
GAPDH	5'ACCACCATGGAGAAGGCTGG 3'	5'CTCAGTGTAGCCAGGATGC 3'

Histology and immunohistochemistry

Each animal's liver was carefully removed, promptly fixed in 10 percent formol saline for 48 hours, and then sectioned into 5 m thick paraffin blocks that were stained with hematoxylin and eosin (H&E), Masson trichrome (MT) to demonstrate collagen fibers^[30].

Bax immunohistochemical staining according to Ramos-Vara et al.^[31]. Using the antigen retrieval technique liver sections were stained. The primary antibody used was an immunoglobulin G (IgG) type for Bax detection (commercial kit CSA, DakoCytomation, Denmark). For the negative control, the primary antibody was replaced with PBS.

Morphometrical measurements

Using a Leica Qwin 500 Image Analyzer Computer System (England), Masson trichrome stained sections and immunohistochemical reaction were morphometrically evaluated at the Pathology Department, Faculty of Dentistry, Cairo University. At a magnification of X 400, collagen fiber area percent in MT-stained sections and Bax immunoreaction optical density were determined. Five randomly selected fields per section, totaling five sections, with eight rats in each group were used to measure each parameter

Statistical Analysis

The SPSS program (version 18 for Windows, SPSS Inc. Chicago, IL, USA) was used to tabulate and analyze the gathered data. Quantitative values were presented as the mean \pm SD. Student's t-test were used to compare group data and their correlations were detected by Pearson's correlation. *P-values* < 0.05 were considered significant.

RESULTS

Curcumin effect on HFD induced changes on body weight gain and serum lipid profile

Twelve weeks of ingesting a HFD significantly increased body weight ($P < 0.001$). Furthermore, there was dyslipidemia in the HFD group, demonstrated by the significantly high TC, TG, LDL-C, and significantly low HDL-C. In group III there was significantly decreased body weight, BMI, serum total cholesterol, triglyceride, LDL-c and VLDL-c while level of HDL was increased (Table 2).

HFD on modulation effect of hepatic iron and hepatic malondialdehyde MDA levels

The HFD (group II) demonstrated a significant elevation of hepatic iron and hepatic MDA levels ($P < 0.01$) when compared to the control group .In group III there was significantly decreased these parameters (Table 2).

Effect of curcumin on HFD induced changes on iron parameters

There was a significant decrease in Hb level, MCH, and SI in the HFD group compared to controls. These changes in iron parameters were ameliorated by curcumin (Table 3).

Serum hepcidin, IL-6, and TNF- α

A significant increase in the mean values of serum hepcidin, IL-6, and TNF- α was observed in the HFD (group II) compared to the control group (Table 2). There was a significant positive correlation between serum hepcidin with BMI, serum cholesterol, triglyceride, AC, LDL, ALT, and AST. Also, there was a significant positive correlation between IL-6 and serum hepcidin, TNF- α , or serum ferritin. There was a significant negative correlation between hepcidin and HDL or albumin (Table 4).

Relative expression of hepcidin, IL-6, and TNF- α in adipose tissue

The mRNA expression of hepcidin, IL-6, and TNF- α were upregulated in HFD when compare to control (Figure 1). There was a significant positive correlation between hepcidin expression in adipose tissue and IL-6 or TNF- α expression (Table 5, Figure 2).

Histopathological analyses of hepatic tissues of the experimental groups

Control liver sections stained with H&E revealed normal hepatic structure; hepatocytes radiated from the central vein. The hepatocytes had central rounded nuclei and acidophilic cytoplasm. Blood sinusoids were seen in between hepatocytic cords. Portal areas were seen at the periphery of the lobules. The bile duct and portal vein were detected as normal structures (Figure 3a,b). The HFD group showed changes in the normal hepatic architecture. The hepatocyte cords were seen around a congested central vein. Some hepatocytes with dark stained nuclei and acidophilic cytoplasm, while others had vacuolated cytoplasm. Fatty infiltration in between hepatocytes and blood sinusoids were congested. The portal area had the bile duct, the hepatic artery, as well as a dilated and congested portal vein. Mononuclear cellular infiltration can be seen in the peri-portal area (Figure 4a,b,c).

Liver section from group III showed nearly normal hepatic architecture. Some hepatocytes had vacuolated cytoplasm, while others had central vesicular rounded

nuclei were observed. Blood sinusoids appeared normal. Portal area with bile duct, hepatic artery and portal vein were detected as nearly normal structure. Few hepatocytes with darkly stained nuclei were still seen (Figure 5a,b).

Control Mallory trichrome stained sections revealed few collagen fibers surrounding the central vein and in the portal area, where the portal vein and bile duct were seen (Figure 6a,b). The HFD group showed markedly increased collagen fibers around the central vein and portal area; around the congested portal vein (Figure 6c,d). Moderate amount of collagen was seen in group III around central vein and in portal area around portal vein (Figure 6e,f).

Bax immunohistochemistry revealed a weak positive Bax reaction in the hepatocyte cytoplasm for the control group (Figure 7a). However, a strong positive Bax immune reaction in the hepatocyte cytoplasm was found in the HFD group (Figure 7b). While group III showed a moderate positive reaction for Bax (Figure 7c).

Statistical and morphometrical results

Optical density of Bax immune reaction and area % of collagen fibers as assessed by image analyzer among the different studied groups revealed that high fat fed diet group showed a significant statistically increase in the mean area percent of collagen fibers and optical density of Bax immune reaction when compared with control group. In group III, highly significant decrease in their levels in comparison to group II (Table. 6).

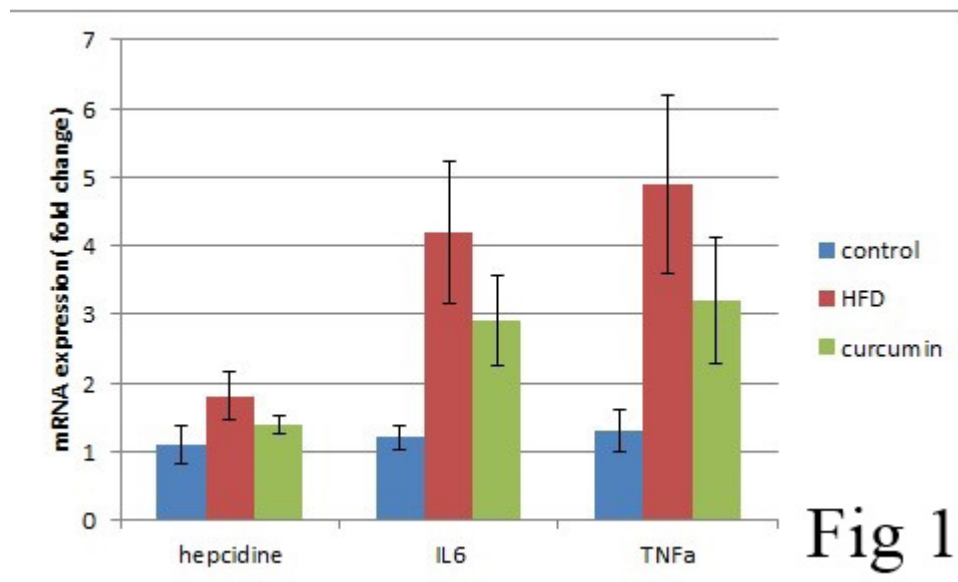


Fig. 1: Adipose tissue hepcidin, IL-6, and TNF- α mRNA expression levels in each study group.

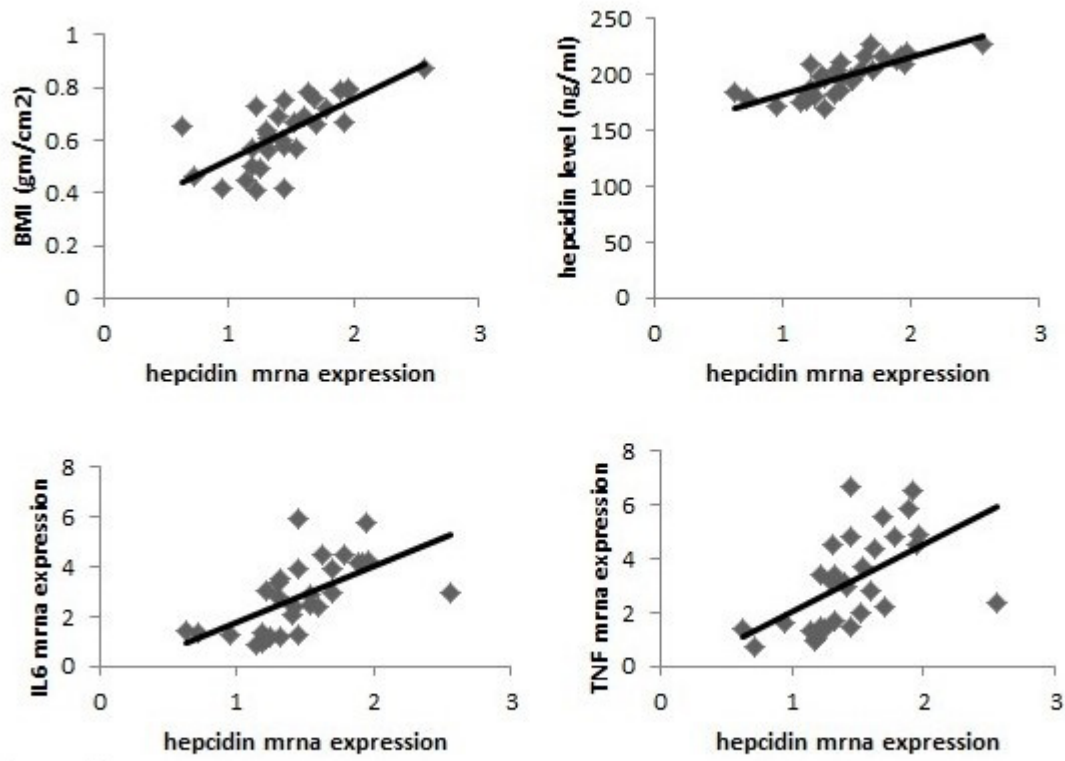


Fig 2

Fig. 2: Correlation between hepcidin gene expression with hepcidin level, BMI, IL-6, and TNF- α expression.

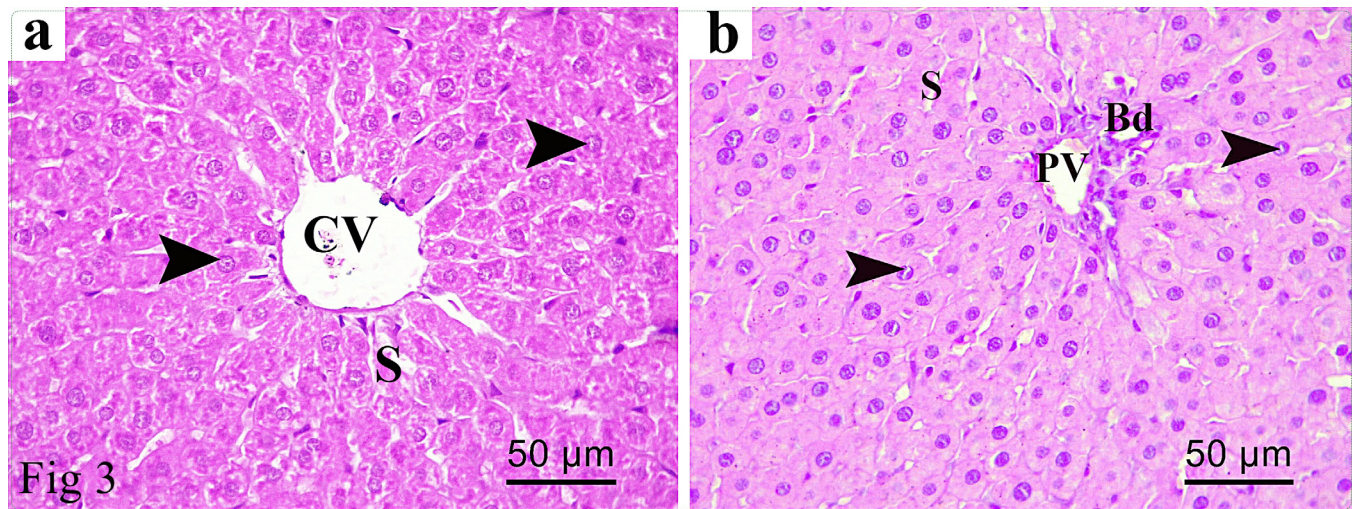


Fig. 3: Photomicrographs of liver section from the control group (a) showing the normal hepatic architecture; central vein (CV) with radiating blood sinusoids (S), hepatocytes arranged in cords with central rounded nuclei (arrowhead), and acidophilic cytoplasm are observed. (b) Showing the portal area with bile duct (Bd) and portal vein (PV) are detected as normal structures. (H&E X 400).

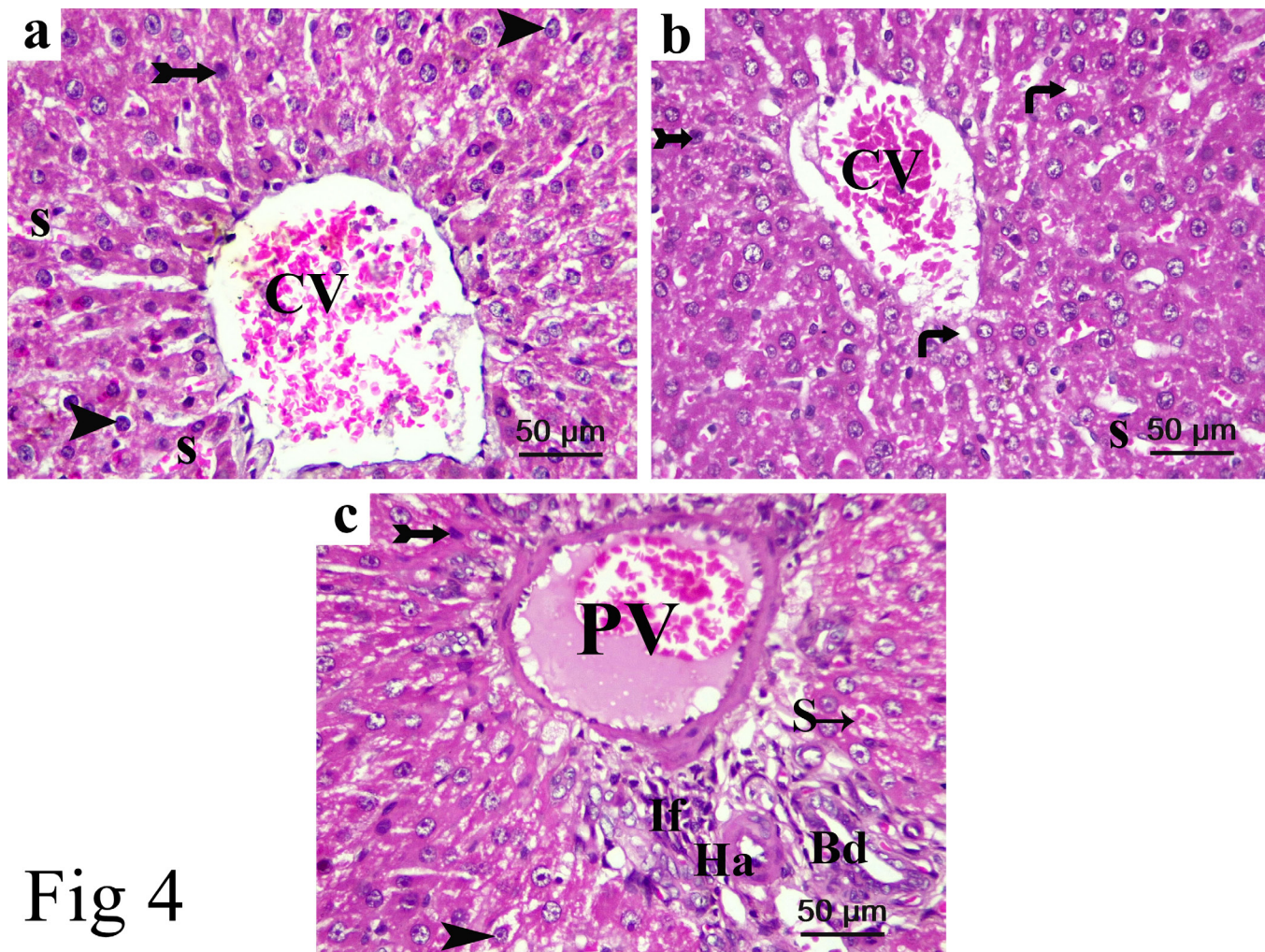


Fig 4

Fig. 4: Photomicrographs of a liver section from group II (a) showing change in the normal hepatic architecture. The hepatocyte cords around the congested central vein (CV) can be seen. Some hepatocytes had dark stained nuclei (bifid arrow) and acidophilic cytoplasm, while others with vacuolated cytoplasm (arrowhead) were observed. Some blood sinusoids appear dilated and congested (S). (b) Some fat cells (curved arrow), congested central vein (CV), some hepatocytes with dark stained nuclei (bifid arrow) and dilated congested blood sinusoids (S) were observed. (c) Showing the portal area with a dilated congested portal vein (PV), bile duct (Bd), and hepatic artery (Ha), dilated congested blood sinusoids (S). Mononuclear cellular infiltration (If) can be seen in the periportal area. (H&E X 400).

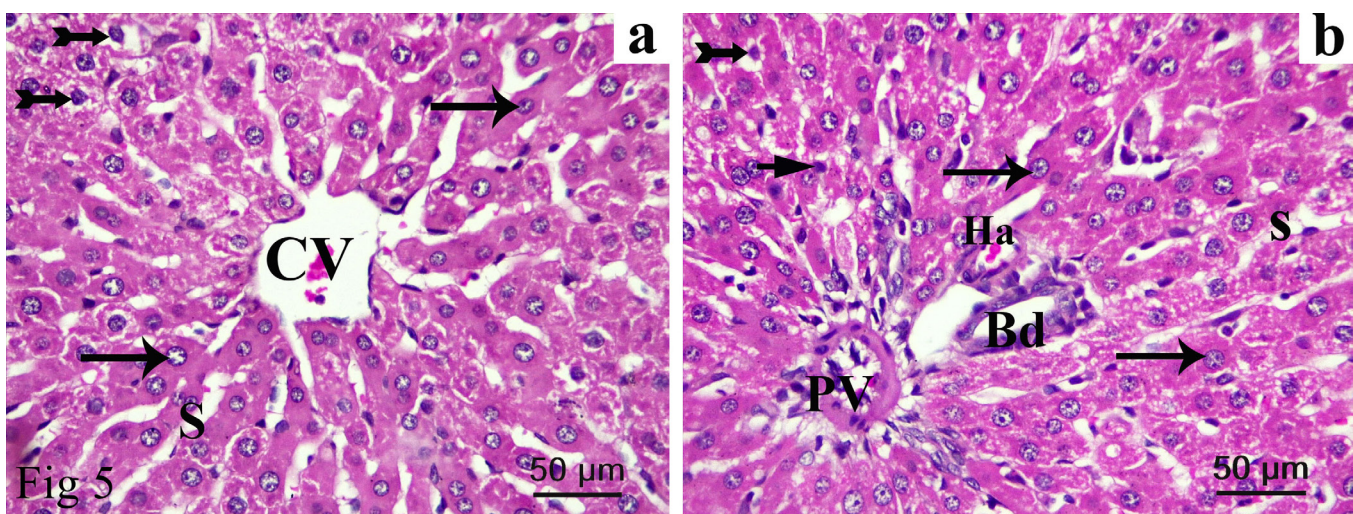


Fig. 5: photomicrograph of a liver section from group III (a) Showing nearly normal hepatic architecture. The cords of hepatocytes around central vein (CV) can be seen. Some hepatocytes with vacuolated cytoplasm (bifid arrow) while others with central rounded vesicular nuclei (arrow) are observed. Blood sinusoids appeared normal (S). (b) Showing the portal area with bile duct (Bd) , hepatic artery (Ha) and portal vein (PV) are detected as nearly normal structure. Few hepatocytes cells with darkly stained nuclei (short arrow) while others with central rounded vesicular nuclei (arrow) are also observed (H&E x400)

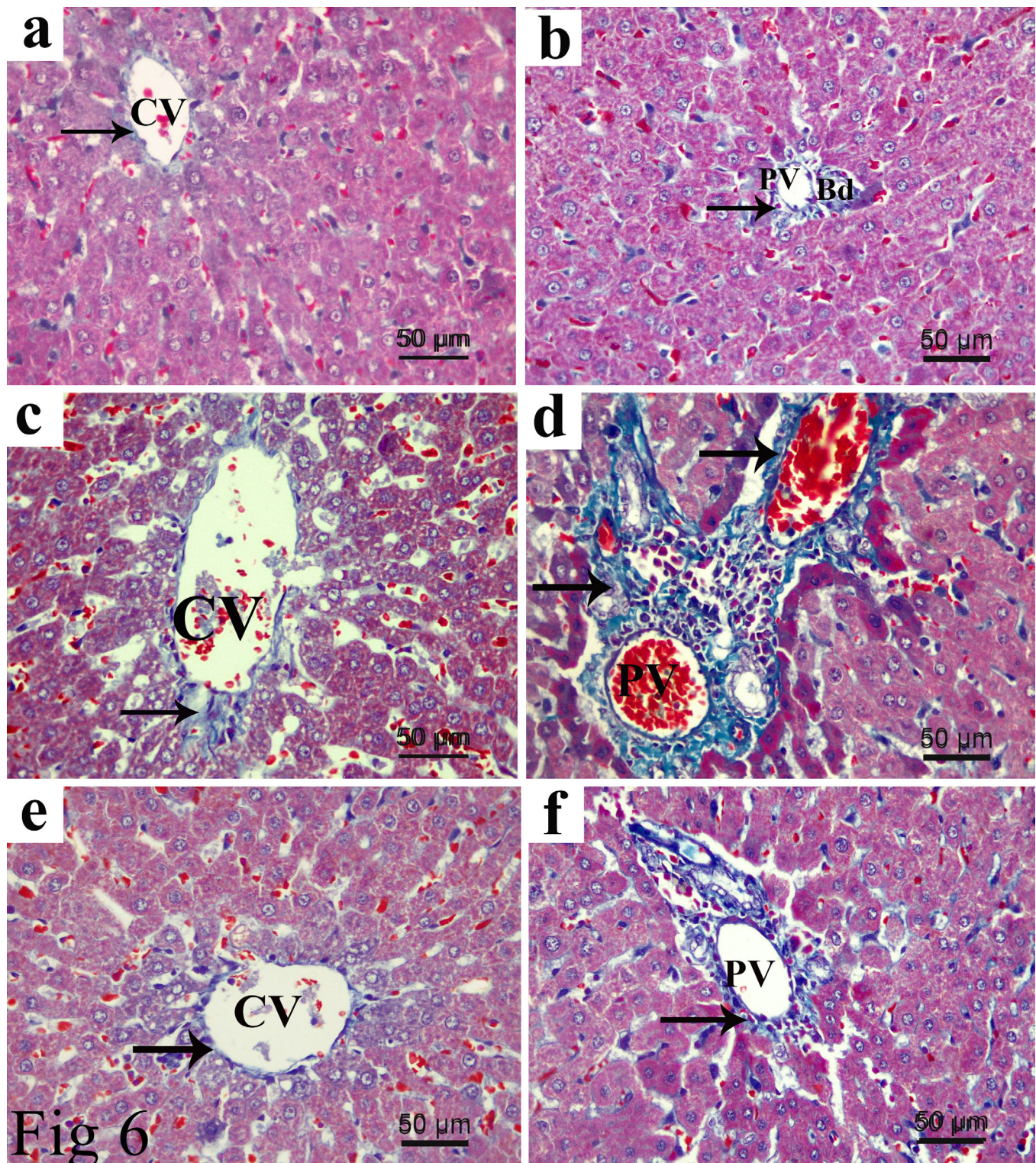


Fig. 6: Mallory trichrome stained sections showing (a and b): few collagen fibers (arrow) around the central vein (CV) and in the portal area. Portal vein (PV) and bile duct (Bd) are seen in the control group. (c and d) A marked increase in collagen deposition around the CV and around congested PV in group II. . (e and f): moderate amount of collagen can be seen in group III, collagen fibers around central vein (CV) and in portal area around portal vein(PV). (MT X 400)

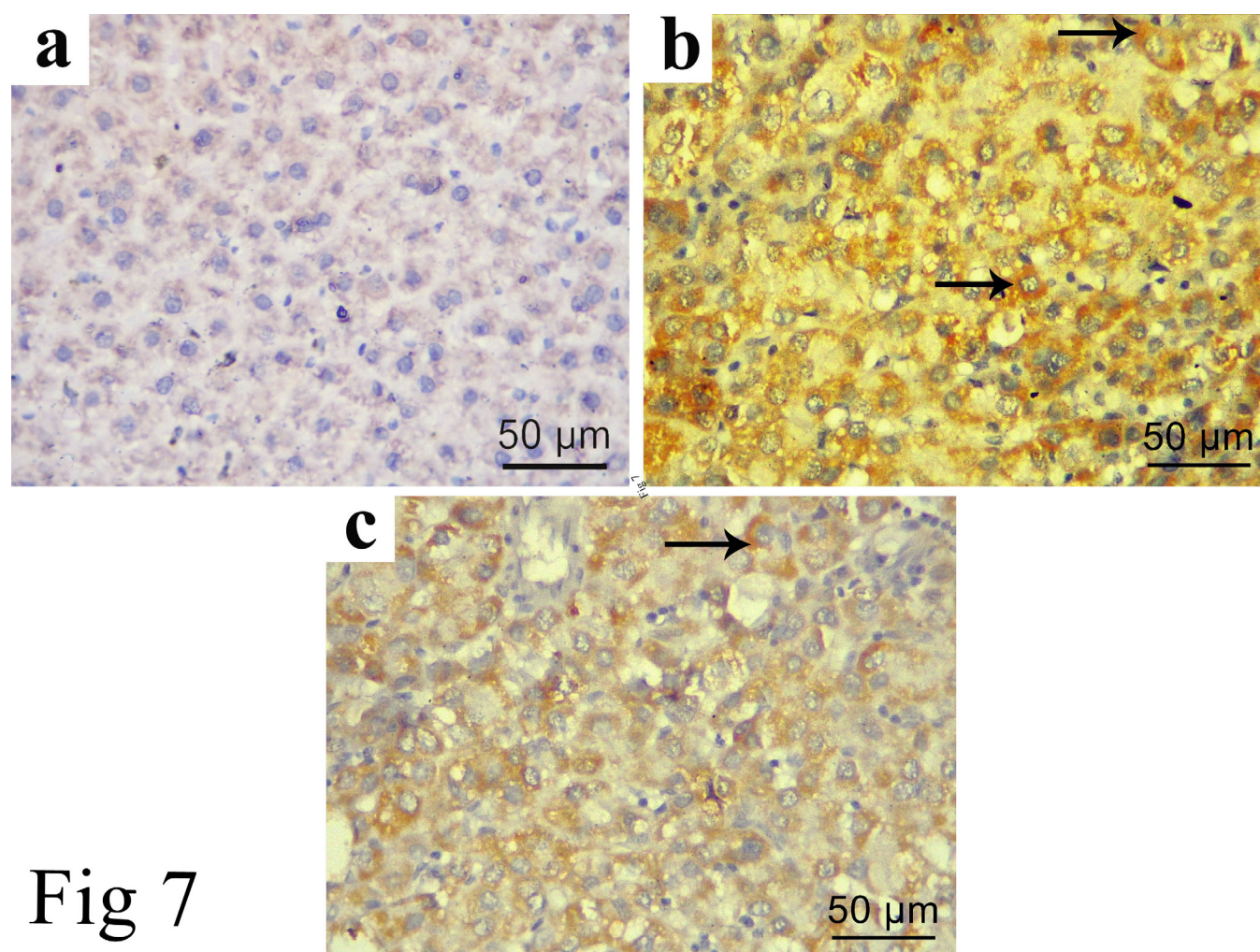


Fig 7

Fig. 7: A photomicrograph of a liver section from the control group. (a) Showing weak positive Bax immune reaction in the hepatocyte cytoplasm. Group II (b) showing strong positive Bax immune reaction in the hepatocyte cytoplasm (arrows). While group III (c) showing a moderate positive reaction for Bax (arrows). (Bax immunostaining X 400)

Table 2: anthropometric and biochemical measurements of all studied groups.

Parameters	Group I	Group II	Group III	<i>P</i> value
Final BMI (gm/cm ²)	0.49 ± 0.07	0.76 ± 0.05 ^a	0.63 ± 0.04 ^{a,b}	< 0.001
AC (cm)	13.43±0.6	24.49±2.7 ^a	18.56±1.9 ^{a,b}	< 0.001
Serum cholesterol (mg/dl)	60.7±7.6	185.3±12.7 ^a	107.1±11.3 ^{a,b}	< 0.001
Serum triglyceride (mg/dl)	53.8±8.6	162.8±10.6 ^a	106.8±8.3 ^{a,b}	< 0.001
Serum HDL-c (mg/dl)	43.7 ± 5.8	19.5 ± 3.2 ^a	36.2 ± 3.9 ^{a,b}	< 0.001
Serum LDL-c (mg/dl)	18.7±4.1	93.9±11.1 ^a	45.2±6.7 ^{a,b}	< 0.001
Serum ALT (mg /dl)	52.1±7.3	134.1±8.5 ^a	86.4±7.8 ^{a,b}	< 0.001
Serum AST (mg /dl)	129.9±6.8	201.9±8.8 ^a	174.5±8.8 ^{a,b}	< 0.001
Serum albumin (g/dl)	5.0±0.68	1.7±0.38 ^a	2.9±0.55 ^{a,b}	< 0.001
Serum Hecpidin (ng/ml)	179.1±6.1	216.7±6.4 ^a	197.7±6.2 ^a	< 0.001
TNF (pg/ml)	12.45±3.98	46.23± 5.89 ^a	19.67±2.45 ^{a,b}	< 0.001
IL6 (pg/ml)	17.59±2.43	33.26 ± 4.92 ^a	20.15 ± 3.74 ^b	< 0.001
Hepatic iron (nmol/mg)	0.14 ± 0.028	0.54 ± 0.11 ^a	0.32±0.12 ^{a,b}	< 0.001
Hepatic MDA (nmol/g)	139.20 ± 4.3	176.5 ± 8.65 ^a	151.4±5.13 ^{a,b}	< 0.001

a = versus group I b = versus groupII NS = non-significant (*P* > 0.05)

Table 3: Iron status parameters in the all studied group

Parameters	Group I	Group II	Group III	<i>P</i> value
Hb (g/d)	12.98±0.9	10.55±0.7 ^a	11.58±0.7 ^{a,b}	< 0.001
PCV (%)	40.9±5.62	36.35±5.26	38.88±3.56	0.1339
MCH (pg)	17.44±1.15	15.0±1.01 ^a	12.61±1.36 ^{a,b}	< 0.001
SI (mg /dl)	171.54±11.54	138.58±3.36 ^a	146.91±5.17	< 0.001
TIBC (mg /dl)	402.39±26.62	313.77±24.51 ^a	359.95±14.27 ^{a,b}	< 0.001
Tsat(%)	30.68±3.62	27.49±4.01	29.12±2.26	0.127
SF (ng/ml)	108.66±22.23	153.65±18.51 ^a	137.69±11.08 ^a	< 0.001

a = versus group I

b = versus groupII

NS = non-significant (*P* > 0.05)**Table 4:** Correlation between hepcidin and serum markers.

Hepcidin (ng/ml)	r	<i>P</i> -value
BMI	0.836	<0.001
AC	0.914	<0.001
Serum Cholesterol (mg/dl)	0.788	<0.001
Serum triglyceride (mg/dl)	0.908	<0.001
HDL (mg/dl)	-0.817	<0.001
LDL (mg/dl)	0.896	<0.001
Serum ALT (mg /dl)	0.903	<0.001
Serum AST (mg /dl)	0.907	<0.001
Serum albumin (g/dl)	-0.818	<0.001
SF	0.740	<0.001
TNF- α (pg/ml)	0.923	<0.001
IL-6 (pg/ml)	0.974	<0.001

r = Pearson's correlation coefficient. *P*-value < 0.05 was considered statistically significant and *P*-value > 0.05 was not considered statistically significant.

Table 6: The optical density of Bax immune reaction and area % of collagen fibers.

Parameters	Group I	Group II	Group III	t-test	<i>P</i> -value
Area % of collagen	1.0±0.3	5.5±1.2	2.0±0.5	14.09	<0.001
Optical density of Bax	1.5±0.1	9.8±2.1	3.5±0.6	15.29	<0.001

P-value < 0.05 was considered statistically significant and *P*-value > 0.05 was not considered statistically significant.

DISCUSSION

Over recent years, the obesity prevalence has rapidly increased, creating a major public health problem^[32]. Obese individuals suffer from a persistent low-grade inflammatory disorder, eventually inducing many subsequent complications. Adipose tissue has a role in hepcidin secretion. Hepatic cells produce 150-fold more hepcidin than fat cells. However, more hepcidin is produced by the adipose tissue owing to its larger mass (60–70 kg) (20-folds higher than hepatic mass in highly obese individuals) 5. Its expression increases in cases of insulin resistance and generalized inflammation, which are common in obese individuals 33.

The present study evaluates the variation in hepcidin expression in adipose tissue after HFD and its role in iron homeostasis, In order to better understand how this role

Table 5: Correlation between hepcidin gene expression with hepcidin level, BMI, IL-6, and TNF- α expression.

Hepcidin mRNA expression	r	<i>P</i> -value
BMI (gm/cm ²)	0.718	<0.001
Serum hepcidin (ng/ml)	0.789	<0.001
IL-6 mRNA expression	0.646	<0.001
TNF- α mRNA expression	0.6152	<0.001

r = Pearson's correlation coefficient. *P*-value < 0.05 was considered statistically significant and *P*-value > 0.05 was not considered statistically significant.

participates in disorders associated with obesity. Expression of hepcidin is reduced by hypoxia, iron shortage, and inefficient erythropoiesis and stimulated by iron overload and inflammation^[33]. The IL-6/STAT3 (Signal Transducer and Activator of Transcription-3) pathway mediates hepcidin production during inflammatory circumstances, such as in obesity^[34].

Hepcidin is responsible for controlling iron homeostasis by inhibiting intestinal absorption and releasing iron from macrophages^[34,35]. The current study showed that rats on HFD had low Hb and iron levels compared to the control group. Additionally, ferritin levels were increased in the HFD group, indicating functional iron deficiency. These results are in agreement with Mehdad et al^[35], who reported that elevated BMI and body fat level were associated with lower hemoglobin concentrations and iron deficiency

anemia. Moreover, Sarafidis et al.^[36] considered obesity as a chronic state of inflammation that can be associated with low serum iron and high serum ferritin^[36].

Accumulating fatty tissue in obese individuals might be responsible for the elevated hepcidin level, which in turn, disturbs iron homeostasis and the synthesis of red blood cells^[37]. This explains the current result, which demonstrates a higher adipose tissue hepcidin expression and the serum levels in the HFD group. These observations are in agreement with many studies, demonstrating abnormally increased serum hepcidin and decreased serum iron in overweight children compared to those with a normal weight^[38,39]. Our results revealed that there was a positive correlation between ferritin and serum hepcidin. Hepcidin induces ferroportin degradation, inhibiting intestinal iron absorption, leading to an accumulation of ferritin in macrophages, hepatocytes and duodenal enterocytes^[36].

To clarify the inflammatory state in adipose tissue, we evaluated the expression of both IL-6 and TNF- α and assessed the correlation between their expression and that of hepcidin. Our results show a high IL-6, TNF- α , and hepcidin mRNA expression in the HFD group. Our results also revealed a positive correlation between IL-6 and TNF- α adipose expression with hepcidin adipose expression (Figure 2). Hepcidin synthesis is increased as a result of an increase in the inflammatory mediators IL-6 and TNF. Hepcidin and IL-6 are both produced and expressed in adipose tissue. Hepcidin can be produced by adipocytes in response to inflammatory stimuli like IL-6^[40].

Bekri et al.^[34], Sanad et al.^[41] and Meyer et al.^[42] all demonstrated that hepcidin mRNA was highly expressed in all obese conditions and that depletion of iron stores modulates hepatic hepcidin production but not adipocytes hepcidin production. However, in our study, we highlight the expression of adipose tissue hepcidin, which is in agreement with Sarafidis^[36]. They credited the stimulated hepcidin production in obese individuals was triggered by adipocyte hypoxia and enhanced the inflammatory cytokines production, such as TNF- α , IL-1, and IL-6. Nemeth et al.^[43] also showed that the production of hepcidin, IL-6, and SI reduction were all directly linked. Also, Bekri and colleagues^[34] reported that hepcidin production and IL-6 or CRP (C-reactive protein) expression by adipocytes were significantly linked.

In our study, we evaluated other obesity-associated complications besides functional iron deficiency. The hepatic histopathological samples of the HFD group revealed hepatic damage presented as fat deposition, mixed inflammatory cell foci, and fibrosis. This could be signs of NASH. Also, the HFD group had significantly low serum albumin, and significantly high ALT and AST.

Histological and immunohistochemical observations support those biochemical results as the HFD rat group revealed changes in the normal hepatic architecture in H&E stained sections. The hepatocyte cords were seen

around a congested central vein. Some hepatocytes with dark stained nuclei and acidophilic cytoplasm, while others had vacuolated cytoplasm. Fatty infiltration between the hepatocytes and congested blood sinusoids were also evident. The portal area had a bile duct, hepatic artery, and a congested dilated portal vein. Mononuclear cellular infiltration can be seen in the peri-portal area. Disturbed hepatic architecture seen in this study was attributed to oxidative protein damage in the liver cells. Additionally, necrotic changes in hepatocytes cause irregularity in the orientation of hepatocyte plate, ultimately disturbing the hepatic architecture^[44]. Congested and dilated central veins, blood sinusoids, and portal veins are attributed to ischemia, inflammatory changes, and hypoxia following HFD^[44]. The dilatation may also be due to developing hypertension after obesity induced by HFD^[45].

It was revealed that adipocytes in the fatty liver are active cells that secrete pro-inflammatory cytokines as: TNF- α , IL-6, and reactive oxygen species (ROS). All of these factors play a role in the hepatocyte damage and chronic inflammatory state^[46]. Furthermore, cytoplasmic vacuolation was a result of lipid peroxidation because of oxidative stress that damaged the cell and organelle membranes, leading to increased permeability and disturbed ion concentrations in the cytoplasm and cell organelles^[47,48].

Masson trichrome stained sections showed that collagen deposition was noticeably increased in the area surrounding the central vein and portal region. Chronic liver injury leads to liver fibrosis, as well as excessive collagen deposition and other extracellular matrix (ECM) components^[49]. ROS generation has an important role in liver damage by enhancing the production of pro-fibrogenic mediators and initiating hepatic fibrogenesis^[50].

We observed a strong positive Bax immune reaction in hepatocyte cytoplasm in HFD rats. While group III showing a moderate positive reaction for Bax. These findings were in agreement with Panasiuk et al.^[51], who found that Bax expression was significantly higher in steatosis hepatocytes in the patients with NAFLD. Panasiuk et al.^[51] also stated that apoptosis is one of the most important mechanisms that can eliminate hepatocytes in NAFLD. The inflammation intensification in NAFLD induces the pro-apoptotic proteins p53 and Bax with the inhibition of anti-apoptotic Bcl-2^[52].

To emphasize the histological finding in hepatic tissue, we evaluated hepatic iron and hepatic MDA. Our results showed that both hepatic iron and MDA levels were significantly increased in the HFD group. This may be explained by iron being stored in the liver mainly as ferritin. It has been reported that iron in the microenvironment can trigger regional oxidative stress and subsequent lipid peroxidation. Elevated oxidative stress in HFD-fed rats indicates hepatic fat accumulation with increased hepatic fatty acids oxidation and macrophage activation. This scenario stimulates the inhibitor NF- κ B in hepatic cells and

increases the expression of pro-inflammatory cytokines, as TNF- α and IL-6. In turn, this leads to enhanced hepatic injury and acceleration to NAFLD development in obese subjects^[53,54].

Another explanation for this link was provided by Sarafidis who stated that HFD precipitated hepatic inflammation, such as injury stimulated release of adipose-derived cytokines and leptin, which are believed to trigger insulin resistance and NAFLD. This eventually stimulates hepatic hepcidin production by a similar mechanism to IL-6^[36].

Also iron localization in obese mice visceral adipose tissues correlated with macrophage infiltration between the adipocytes. The iron retention in these cells also contributes to their production of pro-inflammatory cytokines. Therefore, iron can induce insulin resistance and reduce adiponectin expression in isolated adipocytes^[55].

In this research, Liver section from group III showed nearly normal hepatic architecture. Some hepatocytes had vacuolated cytoplasm, while others with central vesicular rounded nuclei were observed. Blood sinusoids appeared normal. Portal area with bile duct, hepatic artery and portal vein were detected as nearly normal structure. Few hepatocytes with darkly stained nuclei were still seen. These results were in agreement with Feng *et al.*^[56] who found that oral administration of curcumin in HFD-fed mice reduces liver steatosis by lowering plasma dyslipidemia and hepatic triglyceride accumulation, suggesting that curcumin has a protective role on HFD-induced hepatic steatosis and NAFLD.

Curcumin supplementation Inhibit adipocyte angiogenesis, lowering preadipocyte differentiation, and reducing lipid accumulation in adipocytes all contribute to a reduction in body weight^[57].

In this study, it was found that curcumin's protective effects were accompanied by the elimination of oxidative stress, which was exhibited by lowering the elevated level of MDA. These results are in consistence with previously reported studies^[58]. Curcumin's recognized antioxidant actions include inhibiting the production of ROS, scavenging free radicals, and chelating oxidative metals including iron and copper^[59].

This study showed that giving curcumin to HFD-fed rats protected them from developing hepatic disorders. This was shown by an improvement in the activity of the liver enzymes ALT and AST which was supported by an amelioration of the severity grade of liver injury and a decrease in liver index. These findings are quite concerning when compared to other investigations using various animal models of NAFLD, including HFD^[60].

In summary, HFD-induced obesity was associated with adipose tissue inflammation and increased the expression of both IL-6 and TNF- α . This, in turn, stimulated the expression of adipose hepcidin, leading to functional iron deficiency. We also conclude that dysregulation of

iron metabolism may contribute to fatty liver progression associated with obesity. Curcumin ameliorated the development of these abnormalities. The protective effect of curcumin depends on its antioxidant, anti-inflammatory effects as well as on the improvement of obesity. Further studies are necessary to determine the effect of hepcidin administration especially in humans which may ameliorate anemia, offering new tools that are already or will be soon clinically explored for the treatment of specific anemias.

CONFLICT OF INTERESTS

There are no conflicts of interest.

REFERENCES

- Güngör NK. Overweight and obesity in children and adolescents. *Journal of Clinical Research in Pediatric Endocrinology* 2014;6:129-43. doi: 10.4274/Jcrpe.1471.
- Kachur S, Lavie CJ, de Schutter A, Milani RV, Ventura HO. Obesity and cardiovascular diseases. *Minerva Medica* 2017;108:212-28. doi: 10.23736/S0026-4806.17.05022-4.
- Mundi, M.S.; Velapati, S.; Patel, J.; Kellogg, T.A.; Abu Dayyeh, B.K.; Hurt, R.T. Evolution of NAFLD and Its Management. *Nutr. Clin. Pract.* 2020, 35, 72–84. [CrossRef] doi: 10.1002/ncp.10449.
- Cao H. Adipocytokines in obesity and metabolic disease. *Journal of Endocrinology* 2014;220:T47-T59. doi: 10.1530/JOE-13-0339.
- Knutson MD, Oukka M, Koss LM, Aydemir F, Wessling-Resnick M. Iron release from macrophages after erythrophagocytosis is up-regulated by FPN-1 1 overexpression and down-regulated by hepcidin. *Proceedings of the National Academy of Sciences of the United States of America* 2005;102:1324-8. doi: 10.1073/pnas.0409409102.
- Laftah AH, Ramesh B, Simpson RJ, *et al.* Effect of hepcidin on intestinal iron absorption in mice. *Blood* 2004;103:3940-4. DOI: 10.1182/blood-2003-03-0953
- Kirsch R, Sijtsema HP, Tlali M, Marais AD, Hall Pde L. Effects of iron overload in a rat nutritional model of non-alcoholic fatty liver disease. *Liver International* 2006;26:1258-67. DOI: 10.1111/j.1478-3231.2006.01329.x
- Camaschella, C.; Nai, A.; Silvestri, L. Iron metabolism and iron disorders revisited in the hepcidin era. *Haematologica* 2020, 105, 260–272. [CrossRef] • DOI: 10.3324/haematol.2019.232124
- Kumar, S.; Bhatia, P.; Jain, R.; Bharti, B. Plasma hepcidin levels in healthy children: Review of current literature highlights limited studies. *J. Pediatr. Hematol. Oncol.* 2019, 41, 238–242. [CrossRef] DOI: 10.1097/MPH.0000000000001216

10. Z. J. Hawula, D. F. Wallace, V. N. Subramaniam, and G. Rishi, "Therapeutic advances in regulating the hepcidin/ferroportin axis," *Pharmaceuticals*, vol. 12, no. 4, p. 170, 2019. <https://doi.org/10.3390/ph12040170>
11. Amalraj A, Pius A, Gopi S, Gopi S. Biological activities of curcuminoids, other biomolecules from turmeric and their derivatives - a review. *J Tradit Complement Med.* 2017;7:205–33. <https://doi.org/10.1016%2Fj.jtcme.2016.05.005>
12. Maithilikarpagaselvi N, Sridhar MG, Swaminathan RP, Sripradha R. Preventive effect of curcumin on inflammation, oxidative stress and insulin resistance in high-fat fed obese rats. *J Complement Integr Med.* 2016;13:137–43. <https://doi.org/10.1515/jcim-2015-0070>
13. Guerra-Cantera S, Frago LM, Díaz F, Ros P, Jiménez-Hernaiz M, Freire-Regatillo A, Barrios V, Argente J, Chowen JA. Short-Term Diet Induced Changes in the Central and Circulating IGF Systems Are Sex Specific. *Front Endocrinol (Lausanne).* 2020 Aug 11;11:513. PMID: 32849298; PMCID: PMC7431666. <https://doi.org/10.3389/fendo.2020.00513>
14. Svegliati-Baroni G, Candelaresi C, Saccomanno S, et al. Gastrointestinal, hepatobiliary and Pancreatic Pathology-A Model of insulin Resistance and nonalcoholic steatohepatitis in Rats: role of peroxisome proliferator-activated receptor- α and n-3. *American Journal of Pathology* 2006;169:846-60. <https://doi.org/10.2353/ajpath.2006.050953>
15. Hasan ST, Zingg JM, Kwan P, Noble T, Smith D, Meydani M. Curcumin modulation of high fat diet-induced atherosclerosis and steatohepatosis in LDL receptor deficient mice. *Atherosclerosis.* 2014;232:40–51. <https://doi.org/10.1016/j.atherosclerosis.2013.10.016>
16. U m M Y , H w a n g K H , A h n J , H a T Y . Curcuminattenuatesdiet-inducedhepaticsteatosis byactivatingAMP-activatedprotein kinase. *BasicClinPharmacolToxicol.*2013;113:152–7. <https://doi.org/10.1111/bcpt.12076>
17. Novelli EL, Diniz YS, Galhardi CM, et al. Anthropometrical parameters and markers of obesity in rats. *Laboratory Animals* 2007;41:111-9. <https://doi.org/10.1258/00236770779399518>
18. Gerbaix M, Metz L, Ringot E, Courteix D. Visceral fat mass determination in rodent: validation of dual-energy X-ray absorptiometry and anthropometric techniques in fat and lean rats. *Lipids in Health and Disease* 2010;9:140. doi:10.1186/1476-511X-9-140
19. Tietz NW. *Clinical guide to laboratory tests.* 3rd ed. Philadelphia: W B Saunders Co.; 1995. 384-387.
20. Fossati P, Prencipe L. Serum triglycerides determined colorimetrically with an enzyme that produces hydrogen peroxide. *Clinical Chemistry* 1982;28:2077-80. <https://doi.org/10.1093/CLINCHEM%2F28.10.2077>
21. Nauck M, März W, Jarausch J, et al. Multicenter evaluation of a homogeneous assay for HDL-cholesterol without sample pretreatment. *Clinical Chemistry* 1997;43:1622-9. <https://doi.org/10.1093/clinchem/43.9.1622>
22. Friedewald WT, Levy RI, Fredrickson DS. Estimation of the concentration of low-density lipoprotein cholesterol in plasma, without use of the preparative ultracentrifuge. *Clinical Chemistry* 1972;18:499-502. DOI: 4337382
23. Rec JS. Estimation of serum ALT. *Clinical Biochemistry* 1970;8:658.
24. Stoskopf M. *Fish medicine.* USA: Saunders Company; 1993.
25. Xue D, He X, Zhou C. Serum hepcidin level correlates with hyperlipidemia status in patients following allograft renal transplantation. *Transplantation Proceedings.* Elsevier 2014;46:156-9. <https://doi.org/10.1016/j.transproceed.2013.06.020>
26. Amdekar S, Roy P, Singh V, Kumar A, Singh R, Sharma P. Anti-inflammatory activity of lactobacillus on carrageenan-induced paw edema in male Wistar rats. *International Journal of Inflammation* 2012;752015. doi: 10.1155/2012/752015.
27. Burits C, Ashwood E. Methods for the determination of serum iron, iron binding capacity, and transferrin saturation. *Tietz Textbook of clinical chemistry.* 3rd ed. AACC 1999; 1701-3.
28. Siff JE, Meldon SW, Tomassoni AJ. Usefulness of the total iron binding capacity in the evaluation and treatment of acute iron overdose. *Annals of Emergency Medicine* 1999;33:73-6. [https://doi.org/10.1016/s0196-0644\(99\)70420-8](https://doi.org/10.1016/s0196-0644(99)70420-8)
29. Hu X, Jogasuria A, Wang J et al. MitoNEET deficiency alleviates experimental alcoholic steatohepatitis in mice by stimulating endocrine adiponectin-FGF15 axis. *Journal of Biological Chemistry* 2016;291:22482-95. <https://doi.org/10.1074/jbc.m116.737015>
30. Suvarna, K. S., Layton, C., & Bancroft, J. D. (Eds.), (2018): *Bancroft's theory and practice of histological techniques E-Book.* Elsevier Health Sciences. eBook ISBN: 9780702068867
31. Ramos-Vara JA, Kiupel M, Baszler T et al. Suggested guidelines for immunohistochemical techniques in veterinary diagnostic laboratories. *Journal of Veterinary Diagnostic Investigation* 2008;20:393-413. <https://doi.org/10.1177/104063870802000401>

32. Hamza RT, Hamed AI, Kharshoum RR. Iron homeostasis and serum hepcidin-25 levels in obese children and adolescents: relation to body mass index. *Hormone Research in Paediatrics* 2013;80:11-7. <https://doi.org/10.1159/000351941>
33. Albu A, Adipokines LupuD. systemic inflammation and exercise. *Palestrica of the Third Millennium Civilization and Sport* 2015;16. DOI: 10.1080/1744666X.2017.1249850
34. Bekri S, Gual P, Anty R, et al. Increased adipose tissue expression of hepcidin in severe obesity is independent from diabetes and NASH. *Gastroenterology* 2006;131:788-96. <https://doi.org/10.1053/j.gastro.2006.07.007>
35. Mehdad S, Benaich S, Hamdouchi AE, Bouhaddou N, Azlaf M, Menchawy IE, Belghiti H, Benkirane H, Lahmam H, Barkat A, Kari KE, Mzibri ME, Aguenau H. Association between overweight and anemia in Moroccan adolescents: a cross-sectional study. *Pan Afr Med J.* 2022 Feb 22;41:156. doi: 10.11604/pamj.2022.41.156.20927. PMID: 35573439; PMCID: PMC9058990. <https://doi.org/10.11604/pamj.2022.41.156.20927>
36. Sarafidis PA, Rumjon A, MacLaughlin HL, Macdougall IC. Obesity and iron deficiency in chronic kidney disease: the putative role of hepcidin. Oxford University Press; 2011. <https://doi.org/10.1093/ndt/gfr686>
37. Coimbra S, Catarino C, Santos-Silva A. The role of adipocytes in the modulation of iron metabolism in obesity. *Obesity Reviews* 2013;14:771-9. <https://doi.org/10.1111/obr.12057>
38. Stoffel, N.U., El-Mallah, C., Herter-Aeberli, I. et al. The effect of central obesity on inflammation, hepcidin, and iron metabolism in young women. *Int J Obes* 44, 1291–1300 (2020). <https://doi.org/10.1038/s41366-020-0522-x>.
39. Aeberli I, Hurrell RF, Zimmermann MB. Overweight children have higher circulating hepcidin concentrations and lower iron status but have dietary iron intakes and bioavailability comparable with normal weight children. *International Journal of Obesity* 2009;33:1111-7. <https://doi.org/10.1038/ijo.2009.146>
40. Fleming RE. Iron and inflammation: cross-talk between pathways regulating hepcidin. *Journal of Molecular Medicine* 2008;86:491-4. <https://doi.org/10.1007/s00109-008-0349-8>.
41. Sanad M, Osman M, Gharib A. Obesity modulate serum hepcidin and treatment outcome of iron deficiency anemia in children: a case control study. *Italian Journal of Pediatrics* 2011;37:34. <https://doi.org/10.1186/1824-7288-37-34>
42. Meyer LK, Ciaraldi TP, Henry RR, Wittgrove AC, Phillips SA. Adipose tissue depot and cell size dependency of adiponectin synthesis and secretion in human obesity. *Adipocyte* 2013;2:217-26. <https://doi.org/10.4161/adip.24953>
43. Nemeth E, Rivera S, Gabayan V, et al. IL-6 mediates hypoferrremia of inflammation by inducing the synthesis of the iron regulatory hormone hepcidin. *The Journal of Clinical Investigation* 2004;113:1271-6. <https://doi.org/10.1172/jci20945>.
44. Abraham P, Wilfred G, Ramakrishna B. Oxidative damage to the hepatocellular proteins after chronic ethanol intake in the rat. *Clinica Chimica Acta* 2002;325:117-25. [https://doi.org/10.1016/s0009-8981\(02\)00279-6](https://doi.org/10.1016/s0009-8981(02)00279-6).
45. Arvanitidis AP, Corbett D, Colbourne F. A high fat diet doesn't exacerbate CA1 injury and cognitive deficits following global ischemia in rats. *Brain Research* 2009;1252:192-200. <https://doi.org/10.1016/j.brainres.2008.11.058>
46. Elahi MM, Cagampang FR, Mukhtar D, Anthony FW, Ohri SK, Hanson MA. Long-term maternal high-fat feeding from weaning through pregnancy and lactation predisposes offspring to hypertension, raised plasma lipids and fatty liver in mice. *British Journal of Nutrition* 2009;102:514-9. <https://doi.org/10.1017/s000711450820749x>
47. Brunt EM, Tiniakos DG. Histopathology of nonalcoholic fatty liver disease. *World Journal of Gastroenterology* 2010;16:5286-96. <https://doi.org/10.3748/wjg.v16.i42.5286>
48. Panqueva RP. Pathological aspects of fatty liver disease. *Rev Col Gastroenterol* 2014;29:72-8. <https://doi.org/10.1053/j.gastro.2014.07.056>
49. Emanuel R. Essential pathology. 3rd ed. Ch. 1: Lippincott Williams & Wilkins. p. 1; 2001.
50. Friedman SL. Mechanisms of hepatic fibrogenesis. *Gastroenterology* 2008;134:1655-69. <https://doi.org/10.1053/j.gastro.2008.03.003>
51. Mohammed A, Abd Al Haleem EN, El-Bakly WM, El-Demerdash E. Deferoxamine alleviates liver fibrosis induced by CCl4 in rats. *Clinical and Experimental Pharmacology and Physiology* 2016;43:760-8. <https://doi.org/10.1111/1440-1681.12591>.
52. Panasiuk A, Dzieciol J, Panasiuk B, Prokopowicz D. Expression of p53, Bax and Bcl-2 proteins in hepatocytes in non-alcoholic fatty liver disease. *World Journal of Gastroenterology* 2006;12:6198-202. <https://doi.org/10.3748/wjg.v12.i38.6198>
53. Adams PC, Barton JC. A diagnostic approach to hyperferritinemia with a non-elevated transferrin saturation. *Journal of Hepatology* 2011;55:453-8. <https://doi.org/10.1016/j.jhep.2011.02.010>

54. Takaki A, Kawai D, Yamamoto K. Multiple hits, including oxidative stress, as pathogenesis and treatment target in non-alcoholic steatohepatitis (NASH). *International Journal of Molecular Sciences* 2013;14:20704-28. <https://doi.org/10.3390/ijms141020704>
55. Gotardo ÉM, dos Santos AN, Miyashiro RA, et al. Mice that are fed a high-fat diet display increased hepcidin expression in adipose tissue. *Journal of Nutritional Science and Vitaminology* 2013;59:454-61. <https://doi.org/10.3177/jnsv.59.454>
56. Dan Feng, Jun Zou , Dongfang Su, Haiyan Mai, Shanshan Zhang, Peiyang Lil and Xiumei Zheng. Curcumin prevents high-fat diet-induced hepatic steatosis in ApoE^{-/-} mice by improving intestinal barrier function and reducing endotoxin and liver TLR4/NF-κB inflammation *Nutrition & Metabolism* (2019) 16:79. <https://doi.org/10.1016/j.jnutbio.2023.109403>
57. Ejaz A, Wu D, Kwan P, Meydani M. Curcumin inhibits adipogenesis in 3T3-L1 adipocytes and angiogenesis and obesity in C57/BL mice. *J Nutr* 2009; 139:919. doi:10.3945/jn.108.100966.
58. Zhou H, S Beevers C, Huang S. The targets of curcumin. *Curr Drug Targets* 2011; 12:332. <https://doi.org/10.2174/138945011794815356>
59. Masarone M, Rosato V, Dallio M, Gravina AG, Aglitti A, Loguercio C et al. Role of oxidative stress in pathophysiology of nonalcoholic fatty liver disease. *Oxid Med Cell Longev* 2018; 2018:9547613. <https://doi.org/10.1155/2018/9547613>
60. Zhao NJ, Liao MJ, Wu JJ, Chu KX. Curcumin suppresses Notch-1 signaling: Improvements in fatty liver and insulin resistance in rats. *Mol Med Rep* 2018; 17:819-826. <https://doi.org/10.3892/mmr.2017.7980>

الملخص العربي

الركمين يحسن من الاضطرابات المرتبطة بالسمنة في ذكور الفئران البيضاء التي تتغذى على نسبة عالية من الدهون: دور الهيبسيدين

امل فوزي عبد المجيد،^١ رضوى محمود السيد،^٢ صفية ابراهيم اسماعيل،^٣ عبير عبد العظيم محمود،^٤
اولاء محمد سامي

اقسم الكيمياء الحيوية الطبية،^١ قسم الفسيولوجيا،^٢ قسم الأنسجة الطبية وبيولوجيا الخلية، كلية الطب،
جامعة الزقازيق، مصر

خلفية: في البلدان المتقدمة ، كثيرا ما تواجه السمنة ونقص الحديد اضطرابات غذائية. مرض الكبد الدهني غير الكحولي هو مشكلة صحية عالمية. الهيبسيدين هو الببتيد الذي تنتجه بشكل رئيسي خلايا الكبد والخلايا الشحمية ، المسؤولة عن استقلاب الحديد ، والمناعة ، والتنظيم الالتهابي. الركمين ، العنصر النشط للركم.

الهدف من العمل: تقييم دور الهيبسيدين في توازن الحديد وتأثيراته على الكبد الدهني في الفئران البيضاء المصابة بالسمنة التي يسببها النظام الغذائي عالي الدهون. أيضا استكشاف الدور الوقائي للركمين في الاضطرابات المرتبطة بالسمنة المرتبطة بالهيبسيدين.

المواد والطرق: تم تقسيم ثلاثين من ذكور الفئران البيضاء البالغة إلى ثلاث مجموعات: المجموعة الأولى: استهلكت نظاما غذائيا عاديا ، والمجموعة الثانية: استهلكت نظاما غذائيا عالي الدهون وتم تغذية المجموعة الثالثة المعالجة بالركمين بنظام غذائي غني بالدهون مكمل بالركمين. تم قياس مؤشر كتلة الجسم ومحيط البطن وملف الدهون وبعض معلمات الحديد. أيضا ، تم قياس هيبسيدين المعبر عن الأنسجة الدهنية ، إنترلوكين ٦ ، وعامل نخر الورم (TNF) α عن طريق تفاعل البوليميراز المتسلسل في الوقت الفعلي. تم تلطيخ الأنسجة الكبدية بالهيماتوكسيلين والايوسين ، ماسون ثلاثي الألوان وفحصها مجهريا. تم الكشف عن مستويات التعبير عن بروتينات BAX بواسطة الكيمياء الهيستولوجية المناعية.

النتائج: حفز النظام الغذائي الغني بالدهون بشكل كبير تعبير الأنسجة الدهنية من الهيبسيدين و إنترلوكين ٦ وعامل نخر الورم (TNF) α . كان لدى مجموعة النظام الغذائي غني بالدهون حديد مصل منخفض ومستويات تشبع ترانسفيرين وفيريتين مصل مرتفع. كان هناك ارتباط معنوي بين تعبير الهيبسيدين في الأنسجة الدهنية وتعبير إنترلوكين ٦ ، وعامل نخر الورم (TNF) α في مجموعة النظام الغذائي الغني بالدهون. كما تم تحديد الكبد الدهني غير الكحولي في مجموعة السمنة التي يسببها النظام الغذائي الغني بالدهون. العلاج مع الركمين تحسن بشكل كبير المعلمات المذكورة أعلاه.

الخلاصة: يلعب تعبير الهيبسيدين في الأنسجة الدهنية دورا مهما في نقص الحديد الوظيفي والكبد الدهني غير الكحولي في الفئران البيضاء البدينة التي يتم تحسينها بواسطة الركمين الذي له تأثيرات مضادة للسمنة ومضادة للأكسدة ومضادة للالتهابات.